^{110m}In-DTPA-D-Phe^{1}-Octreotide for Imaging of Neuroendocrine Tumors with PET

Mark Lubberink, PhD[1,2]; Vladimir Tolmachev, PhD[1]; Charles Widström, MSc[2]; Alexander Bruskin, PhD[3]; Hans Lundqvist, PhD[1]; and Jan-Erik Westlin, PhD, MD[1]

[1]*Department of Oncology, Radiology, and Clinical Immunology, Uppsala University, Uppsala, Sweden;* [2]*Department of Hospital Physics, Uppsala University Hospital, Uppsala, Sweden; and* [3]*Institute of Theoretical and Experimental Physics, Moscow, Russia*

The somatostatin analog diethylenetriaminepentaacetic acid (DTPA)-D-Phe^{1}-octreotide labeled with ^{111}In has been applied extensively for diagnosis of neuroendocrine tumors using SPECT or planar scintigraphy. However, the spatial resolution of planar scintigraphy and SPECT prohibits imaging of small tumors, and the quantification accuracy of both methods is limited. **Methods:** We developed a method to prepare the positron-emitting radiopharmaceutical ^{110m}In-DTPA-D-Phe^{1}-octreotide based on a commercially available kit. Phantom studies were done to investigate and compare the performance of ^{110m}In PET and ^{111}In SPECT. A clinical imaging study using ^{110m}In-DTPA-D-Phe^{1}-octreotide and PET was done to investigate the application of this radiopharmaceutical. **Results:** An almost 3-fold better resolution and much better quantitative capabilities were found for ^{110m}In PET than for ^{111}In SPECT. The clinical imaging study demonstrated the potential use of ^{110m}In-octreotide in PET to image tumors and quantify radioactivity uptake in humans using ^{110m}In-DTPA-D-Phe^{1}-octreotide. **Conclusion:** PET with ^{110m}In-DTPA-D-Phe^{1}-octreotide greatly improved detection of small tumors and offers a possibility of more accurate quantification of tumor uptake than can be obtained with ^{111}In-DTPA-D-Phe^{1}-octreotide and SPECT.

Key Words: PET; SPECT; ^{110m}In; ^{111m}In; octreotide

J Nucl Med 2002; 43:1391–1397

Today, about 50% of all malignant tumors can be successfully treated with surgery, external radiotherapy, and chemotherapy. The remainder are mainly tumors that have extensively spread and have metastatic growth. Further improvement in treatment requires effective methods to seek and eradicate spread tumor cells. A promising approach for both diagnostics and therapy is the targeting of tumor-specific cell-surface structures with radiopharmaceuticals. Receptors for the neuropeptide somatostatin are overexpressed in several neuroendocrine tumors, making these receptors potential targets for radionuclide diagnostics and therapy (*1*,*2*). Somatostatin is unstable in vivo and is therefore not suitable for application to diagnostic imaging. Octreotide, an octapeptide analog of somatostatin, has a longer biologic half-life, which makes it more suitable for labeling and imaging. Octreotide can be radioiodinated (*3*) or labeled with the radiometals ^{111}In, ^{67}Ga, ^{64}Cu, ^{90}Y, and ^{161}Tb (*4*–*8*). A kit for preparation of ^{111}In-diethylenetriaminepentaacetic acid (DTPA)-D-Phe^{1}-octreotide, or ^{111}In-octreotide, is commercially available (OctreoScan; Mallinckrodt Medical BV, Petten, The Netherlands), and in recent years, ^{111}In-octreotide has been used extensively in the diagnosis of hormone-producing tumors using planar gamma camera imaging and SPECT (*9*–*13*).

The spatial resolution obtainable with single-photon imaging limits its capability to detect, for example, gastroenteropancreatic tumors. These tumors are frequently small (<1 cm) and difficult to find even with ^{111}In-octreotide scintigraphy (*14*,*15*). For this reason, PET, which has better spatial resolution, has been suggested as a possible way to improve detection of small lesions (*16*). Octreotide has been labeled with the positron-emitting nuclides ^{18}F, ^{68}Ga, and ^{86}Y (*8*,*17*). We propose the use of a short-lived positron-emitting isotope of indium, ^{110m}In (half-life, 69 min), for labeling DTPA-D-Phe^{1}-octreotide using the OctreoScan kit. There is a lack of consensus about the use of the designation "m" in this isotope and in the other ^{110}In isotope (half-life, 4.9 h), but in this article, we follow the notation of Chu SYF et al. (*18*). Because of its short half-life, ^{110m}In is suitable for the labeling of short peptides with fast kinetics, such as octreotide. ^{110m}In-octreotide PET should be able to provide quantitative information about receptor kinetics and concentrations with better temporal and spatial resolution than can ^{111}In-octreotide SPECT. ^{110m}In can be produced either from a ^{110}Sn/^{110m}In generator or using the ^{110}Cd(p,n)^{110m}In nuclear reaction on low-energy cyclotrons, which are available at many PET centers (*19*,*20*). Table 1 shows decay properties for ^{110m}In and ^{111}In.

The aim of this study was to establish a technique for labeling DTPA-D-Phe^{1}-octreotide with ^{110m}In, to compare the performance of ^{110m}In PET and ^{111}In SPECT, and to demonstrate the use of ^{110m}In-octreotide in a clinical imaging study. The Ethics Committee and the Isotope Commit-

Received Dec. 31, 2001; revision accepted Jun. 11, 2002.

For correspondence or reprints contact: Mark Lubberink, PhD, Uppsala Research Imaging Solutions AB, Uppsala University Hospital, 751 85 Uppsala, Sweden.

E-mail: mark.lubberink@pet.uu.se

TABLE 1
Main Decay Radiation of ^{110m}In and ^{111}In

Isotope	Half-life	Radiation	Energy (keV)	Abundance (%)
^{111}In	2.8 d	γ	245.4	94
			171.3	90.2
		Auger	2.72	98
			19.3	15.6
		Conversion electrons	144.6	7.8
		X-ray	23.2	44.3
			23.0	23.5
			26.1	14.5
^{110m}In	69.1 min	β^+, total	1,010 (maximum, 2,260)	62
		γ	657.8	98
		Auger	2.72	33.5
			19.3	5.3
		X-ray	23.2	15
			23.0	8

Data are for positrons, γ-radiation, Auger and conversion electrons, and x-rays with abundances > 5%.

tee of the Uppsala University Medical Faculty approved the patient study, and informed consent was obtained from the patient.

MATERIALS AND METHODS

Production of Radiopharmaceuticals

^{110m}In was produced by irradiating an enriched ^{110}Cd target using the ^{110}Cd(p,n)^{110m}In nuclear reaction according to a previously described method (*20*). In a typical production run, 4 isotopically enriched ^{110}Cd foils (thickness, about 50 μm; Teknowledge UK Ltd., London, U.K.) were irradiated on a water-cooled copper backing at the MC17 cyclotron (Scanditronix AB, Uppsala, Sweden) at Uppsala University PET Centre. An aluminum energy degrader with a thickness of 0.18 g/cm^2 was used to decrease the energy of incident protons to 11.8 MeV (the threshold energy for formation of ^{109}Cd). Beam currents of up to 15 μA were applied for the production of ^{110m}In.

For separation, the irradiated foils were heated at 306°C during 30 min in an argon atmosphere. After cooling, the surface of the foils was etched with 5 mL of 0.05 mol/L HCl. Each foil was then rinsed with 20 mL of deionized water and 20 mL of absolute ethanol and, after drying, was used for further irradiation. The acidic solution of ^{110m}In was evaporated almost to dryness and then was redissolved in 0.6 mL of 4 mol/L HCl and passed through a column with anion-exchange resin (AG 1 × 8, 200–400 mesh; Bio-Rad Laboratories, Hercules, CA) preequilibrated with 4 mol/L HCl. The ^{110m}In was eluted with 5 mL of 0.05 mol/L HCl, and the eluate was evaporated to dryness. ^{110m}In was redissolved in 400 μL of 0.02 mol/L HCl and used for further labeling.

^{110m}In-octreotide was produced using the OctreoScan kit. The labeling of octreotide was performed using a procedure similar to that recommended by the manufacturer for production of ^{111}In-octreotide. ^{110m}In (500 MBq in 0.02 mol/L HCl) was added to a vial containing 10 μg DTPA-D-Phe^1-octreotide. After 30 min of incubation, the content of the vial was diluted with saline. Finally, the product was sterilized by filtration with a 0.22-μm sterile filter (Millipore, Molsheim, France). Analysis of the radiopharmaceuticals was performed using instant thin-layer chromatography (ITLC-SG; Gelman Instrument Co., Ann Arbor, MI), with sodium citrate (0.1 mol/L, pH 5) as the mobile phase. Complementary analysis using Sep-Pak C-18 (Waters, Milford, MA) and size-exclusion high-performance liquid chromatography was also performed. Details on this step were published previously (*21*). Hydrochloric acid of *pro analysi* quality (Merck KGaA, Darmstadt, Germany) was used to prepare the solution. All solutions were prepared with ultrapure water (18 MΩ/cm^3 resistance). All vessels and glassware used in separations were rinsed with concentrated HCl, kept overnight filled with a mixture of ethanol and 3 mol/L HCl (1:1), and rinsed 6 times with ultrapure water before use. Radioactivity was measured with an ultrapure germanium detector (EG&G Ortec, Oak Ridge, TN) online with an 8,192-channel personal computer–based multichannel analyzer (The Nucleus, Oak Ridge, TN). The detector was calibrated for energy and efficiency with a standard ^{152}Eu source of known absolute radioactivity. Deadtime losses were always less than 10% during measurements.

Tomographs

The PET measurements were made with a whole-body scanner (4096+ WB; General Electric Medical Systems, Uppsala, Sweden). This tomograph consists of 8 detector rings, each having 512 bismuth germanate detectors separated by nonremovable septa, producing 15 image planes. The axial field of view (FOV) is 10.4 cm, and the transverse FOV is 55.5 cm. The detection energy threshold is 300 keV. Attenuation can be corrected either analytically, by contour finding or by definition of an ellipse contour, or on the basis of a transmission scan with a rotating ^{68}Ge/^{68}Ga pin source. Before reconstruction by filtered backprojection, corrections for dead time, random coincidences, normalization, scatter, and attenuation were applied. Scatter was corrected using the convolution-subtraction method (*22*). All images were reconstructed using a 4.2-mm Hann filter and a pixel size of 2 mm.

For SPECT measurements, a dual-head system (DynaScan; Picker International, Cleveland, OH) containing two 36 × 36 cm planar NaI detectors applied with medium-energy general-purpose collimators was used. For all phantom measurements, the distance between detectors was kept constant at 46 cm, the minimum possible distance for the resolution phantom. Counts were acquired at 64 angles during 20 s to 2 min for each angle, depending on

counting rate. Detection energy windows were set at 20% around the ^{111}In peaks at 171 and 245 keV. The data acquired in these windows were corrected for scattered radiation using a triple-energy window with data from two 3-keV-wide windows located just below the 171-keV window and centrally between the 171 and 245 keV windows. After scatter correction, the data acquired in both windows were summed. Attenuation was corrected analytically using an ellipse-shaped contour and a linear attenuation correction coefficient of 0.14 cm^{-1}. Projections were filtered using a Metz filter of order 13 before reconstruction by filtered back-projection to 64 image planes of 128 × 128 pixels each, a pixel size of 2.9 mm, and a slice separation of 5.8 mm.

Performance Measurements

Spatial Resolution. A 5 × 45 × 20 cm (height × length × width) polythene block containing a 1-mm-diameter catheter crossing the block at 0, 5, 10, and 20 cm from its center was placed centrally in the FOV of the scanner. Polythene was chosen because of its 0.97 g/cm^3 density, which resembles normal tissue. The catheter was filled with a solution containing approximately 30 MBq of ^{110m}In or ^{111}In, and a 15-min (PET) or 32-min (SPECT) emission scan was made. Transverse resolution was calculated as the mean of the full widths at half maximum of a gaussian fit to a vertical and horizontal profile through the peaks in each image plane. Scatter and attenuation corrections were omitted in the SPECT measurement.

Correction Accuracy. A 20-cm-diameter cylindric polystyrene phantom filled with a solution of approximately 40 MBq of ^{110m}In or ^{111}In was placed in the center of the FOV of the scanner. The phantom contained a 5-cm-diameter cylinder filled with cold water and placed 5 cm above the phantom axis. A 1-h (PET) or 2.1-h (SPECT) emission scan was made. Images were reconstructed both with and without scatter correction. The residual correction error was calculated by dividing the measured radioactivity concentration in a 3-cm-diameter volume of interest through each image plane (PET), or in 15 central image planes (SPECT) inside the cold insert, by the mean radioactivity concentration in six 3-cm-diameter volumes of interest in the same planes in the radioactive solution.

Recovery. A water-filled phantom containing 6 hot spheres with diameters ranging from 11 to 38 mm was placed centrally in the FOV of the scanner. The spheres were filled with a solution containing approximately 1 MBq/mL ^{110m}In or ^{111}In, and a 20-min emission scan was made. Analytic attenuation correction was done. After reconstruction, 10-mm-diameter regions of interest (ROIs) were drawn in each sphere. Because of the large sphere size relative to the spatial resolution, the recovery in the largest sphere was assumed to be 1 for PET. Sphere recovery was calculated by dividing the measured radioactivity concentration in each sphere by the radioactivity concentration in the largest sphere (PET) or the known radioactivity concentration (SPECT).

Clinical Imaging Study

Imaging. To 1 patient who had a small-intestine-carcinoma metastasis in the upper thorax, approximately 175 MBq of ^{111}In-octreotide were administered. A standard clinical SPECT measurement (64 angles, 40 s per angle) was made 24 h after administration. Images were reconstructed as described above, without scatter correction. To the same patient, 140 MBq of ^{110m}In-octreotide were administered intravenously. PET emission scans of the upper thorax were made during the first 50 min after administration. The scan lengths were 1 min (0–5 min after administration), 3 min (5–20 min after administration), and 5 min (20–50 min after administration). The patient was then moved, and two 10-min scans of the lower part of the body, including the kidneys, were made. The patient was moved back to the initial position, and 3 more scans of 10 min each were made at 102, 112, and 122 min after administration. Before all 3 scanning series, a 10-min transmission scan was made for attenuation correction and to verify proper positioning. Images were reconstructed as described above, with scatter correction.

Kinetics. Thirteen blood samples were taken during the first 50 min after administration of ^{110m}In-octreotide, and the blood radioactivity was measured in well counters. The image data in the last 3 PET emission scans were summed before ROIs were drawn. In the summation image, an ROI was drawn around the central tumor at 50% of the maximum radioactivity concentration and was transferred to all individual images. The same procedure was followed for the 16 scans from the first 50 min. Two circular ROIs with radii of 25 mm were drawn at 50 mm from the left and right sides of the tumor to determine the background radioactivity concentration in tissue. All these ROIs were drawn in the 3 planes where the tumor was most visible, and the ROIs in these 3 planes were linked to create volumes of interest for better statistics. ROIs around the kidneys were also drawn at 50% of the maximum radioactivity concentration. The standard uptake values of the central tumor, the blood, and the kidneys were calculated by dividing the tissue radioactivity concentration by the injected radioactivity per kilogram of body weight.

RESULTS

Production of Radiopharmaceuticals

A 1-h-long irradiation of the stacked foil target produced ^{110m}In in excess of 20 GBq. Decay-corrected separation yields were 63%–68%. Labeling, which was performed according to the OctreoScan instructions, gave yields of 93%–98%, as confirmed by independent measurements with instant thin-layer chromatography, Sep-Pak, and high-performance liquid chromatography.

Performance Measurements

Figure 1 shows the spatial resolution as an average of the radial and tangential resolutions in all slices for ^{110m}In PET and

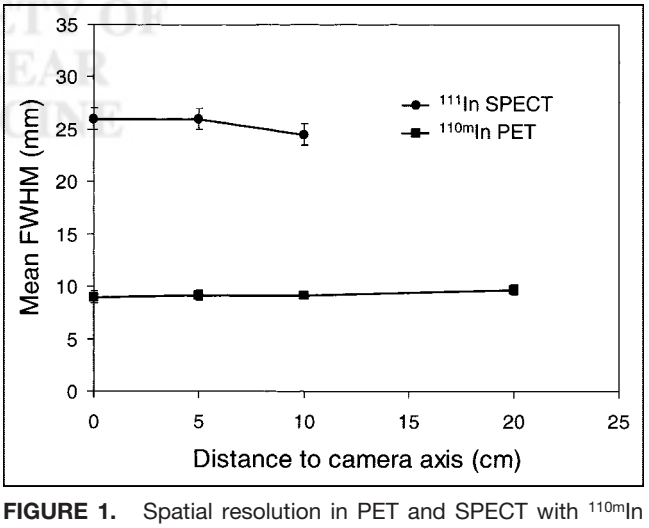

FIGURE 1. Spatial resolution in PET and SPECT with ^{110m}In and ^{111}In, respectively. Just outside FOV in SPECT measurement was 20-cm point. FWHM = full width at half maximum.

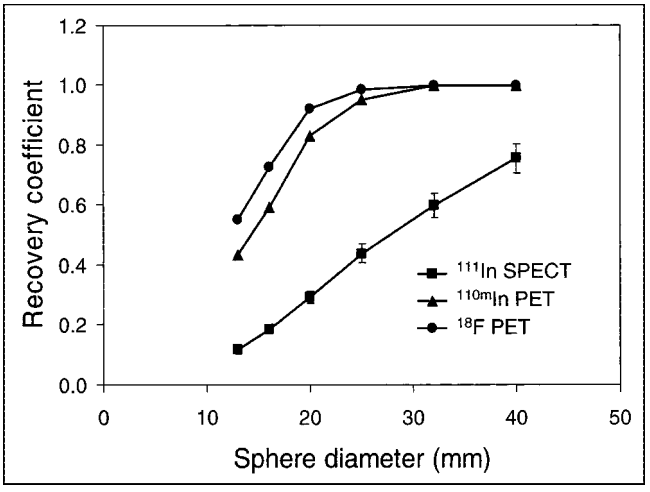

FIGURE 2. Sphere recovery functions for ^{110m}In PET, ^{111}In SPECT, and ^{18}F PET.

in five 5.8-mm-thick slices for ^{111}In SPECT. The residual correction error in the reconstructed images, after attenuation correction in PET and SPECT, was approximately 15% in PET and 31% in SPECT. After scatter correction, the residual correction error was approximately 6% in PET and 26% in SPECT. Figure 2 gives the recovery functions. Recovery in the largest sphere was 76% in SPECT, and recovery in a 20-mm-diameter sphere was 29% for ^{111}In SPECT, compared with 83% for ^{110m}In PET and 93% for ^{18}F PET.

Clinical Imaging Study

SPECT images at 24 h after administration of ^{111}In-octreotide are given in Figure 3. Figure 4 shows PET images taken approximately 1.5 h after administration of ^{110m}In-octreotide. The standard uptake values, calculated from the PET data, are given in Figure 5. The images clearly show that the tumor contour is seen better with PET than with SPECT using standard clinical settings.

DISCUSSION

Our initial labeling experiments confirmed that ^{110m}In-DTPA-D-Phe^1-octreotide can easily be prepared using the OctreoScan kit and locally produced ^{110m}In. The availability of the commercial OctreoScan kit solves problems associated with good-manufacturing-practice production of the peptide–chelator conjugate, and OctreoScan is optimized for labeling with indium isotopes. The radionuclidic purity of the produced ^{110m}In met all requirements for human use, and the production rate gave a sufficient amount of radiopharmaceutical for several patients in 1 production run. The low energy required for the ^{110}Cd(p,n)^{110m}In reaction makes it possible to use any commercially available cyclotron for local production of ^{110m}In. The half-life of ^{110m}In also opens the possibility of delivering the compound to satellite PET centers that do not have their own cyclotron for radionuclide production.

The performance studies clearly showed the improvement in resolution and recovery that can be obtained with ^{110m}In PET in comparison with ^{111}In SPECT. An improvement in resolution by almost a factor 3 would meet the demands of imaging small tumors or metastases (<1 cm) as expressed in the literature (*23,24*). The sphere recovery measurements also showed that quantification is possible in structures with diameters of less than 2 cm. The poorer SPECT recovery, 76% in the largest sphere, was caused mainly by the difference in scatter contribution in the calibration and sphere recovery measurements. The calibration images contained approximately 26% scatter, even after scatter correction, whereas the scatter contribution in the sphere phantom images was much lower because of the distribution of scatter over whole images, not just the spheres, leading to an underestimation of activity concentration in the spheres. The amount of scatter in SPECT measurements causes a major problem in quantification, which can be improved by applying scatter corrections. However, the triple-energy-window scatter correction used here requires good count statistics in the narrow scatter windows and, thus, long measurement times. Kaplan et al. (*25*) suggested a method for ^{111}In SPECT scatter correction based on energy spectrum fitting. Their method, although significantly increasing noise, decreased the measured scatter contribution in their images from 32% to 8%. Another factor introducing quantification problems in SPECT mea-

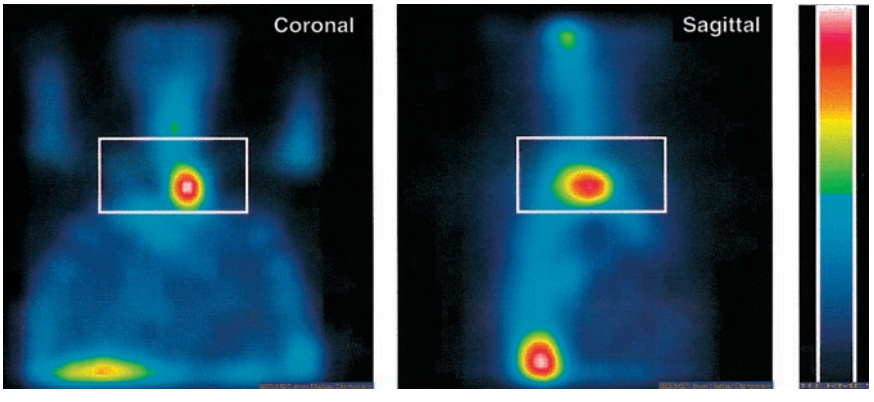

FIGURE 3. Reoriented reconstructed SPECT images 24 h after administration of 175 MBq of ^{111}In-octreotide. Rectangles indicate position of PET images in Figure 4.

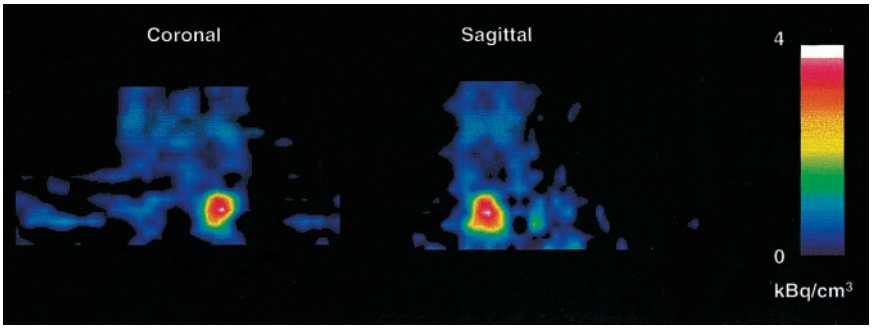

FIGURE 4. Reoriented PET images of same patient as in Figure 3, 1.5 h after administration of ^{110m}In-octreotide.

surements is the applied uniform attenuation correction, which leads to overestimation of radioactivity concentrations in the lungs and underestimation in the bones. Compared with the 1% correction error for the pure positron emitter ^{18}F, the correction error for ^{110m}In PET increased (*26*). This increase was caused by essentially true coincidences involving γ-radiation emitted in the decay of ^{110m}In. The PET scanner cannot distinguish between coincidences involving the 658-keV photon emitted in the ^{110m}In decay and coincidences involving 511-keV photons only. Correction methods for this effect have been suggested (*27–29*) but were not implemented at the time of this study.

The clinical imaging study shows that ^{110m}In-octreotide can be used in studies with PET. The 69-min half-life of ^{110m}In well matches the rapid kinetics of octreotide. The images and uptake curves clearly show the fast blood clearance and kidney uptake of ^{110m}In-octreotide. Kinetics were followed for only up to 2 h, but a measurement time of 4 h should be possible without increasing patient dose. The patient study showed a fast blood clearance phase, with a half-life of approximately 5 min, followed by a slower phase, fast initial uptake in the tumor, and a tumor-to-background uptake ratio of 8 after only 2 h. Even though the energy emitted per decay of ^{110m}In is 2.2 MeV, compared with 438 keV for ^{111}In, the effective dose resulting from a PET study with several hundreds of megabecquerels of ^{110m}In-octreotide would be significantly smaller than the effective dose of an ^{111}In-octreotide administration because of the much shorter half-life of ^{110m}In.

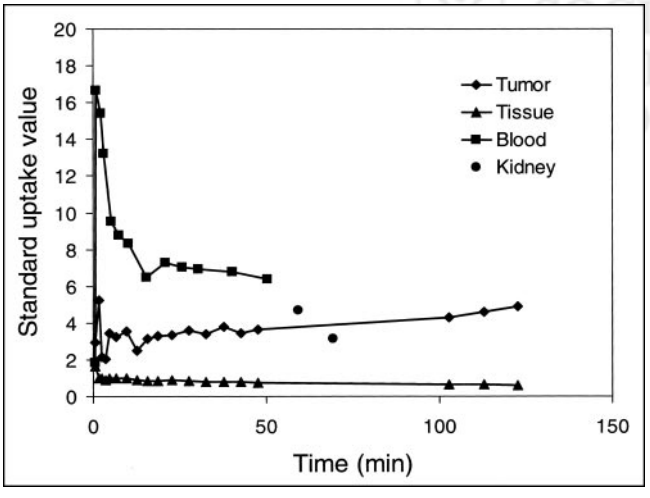

FIGURE 5. Standard uptake values of ^{110m}In-octreotide in tumor, background tissue, blood, and kidney. Error bars are of same size as markers.

^{111}In-labeled octreotide has also been proposed and evaluated for radionuclide therapy using the Auger and conversion electrons emitted in its decay (*30–33*). Dose planning, advanced calculation of dose distribution, and dose monitoring during therapy are prerequisites for successful external therapy. We believe that this same approach is needed if targeted radionuclide therapy is to become successful. Because dose planning is necessary in each patient, there is a need to estimate the spatial and temporal distribution of the therapeutic radionuclide before therapy. During therapy, actual uptake of the radionuclide in tumor and critical organs needs to be determined in order to obtain the radioactivity integral and thus the absorbed dose as accurately as possible. Introduction of the positron-emitting analog ^{110m}In might help to obtain more precise values of the radioactivity concentration in tumors and the critical organs of a given patient and thus aid in the optimization of the therapeutic regimen. This concept has also been suggested for the isotopic analogues ^{90}Y/^{86}Y (*34*) and ^{131}I/^{124}I (*35,36*), and several approaches for dosimetric calculations have been published (*37–39*). Similar half-lives of the positron-emitting and therapeutic isotopes facilitate calculation of the radioactivity integral, which is needed to obtain a good estimate of the absorbed dose. Such a similarity in half-life exists for the isotopic pairs ^{90}Y/^{86}Y and ^{131}I/^{124}I but not for ^{111}In/^{110m}In (Table 1). However, the half-life of ^{110m}In is long enough to measure the first hours of the octreotide kinetics in the individual patient, after which a stationary situation may have become established. The later distribution, measured by gamma camera techniques, can then be related to the early, detailed quantitative PET measurements. Although PET gives a spatial resolution of less than 1 cm^3, only macroscopic dose information is obtained, which is sufficient in healthy tissue. An important part of the dose delivered by ^{111}In is due to the Auger electrons or the conversion electrons emitted in its decay. Biopsies and other studies have to be added if a more detailed dosimetry on the cellular level is wanted. However, being able to determine

an accurate macroscopic dose is an important and necessary first step to beginning to understand the dose–effect relationship of this type of therapy.

Treatment with nonlabeled octreotide is helpful in controlling clinical symptoms through hormone hypersecretion inhibition in most patients with metastatic carcinoids, gastrinomas, insulinomas, and glucagonomas (*40*). However, evidence has been found that this kind of treatment may cause downregulation of the somatostatin receptors in tumor cells (*24*). Quantitative assessment of somatostatin receptor density may be useful in such tumors to evaluate the rationale for somatostatin therapy and to monitor the effect of treatment. The short half-life of ^{110m}In, which allows repeated investigations, is here useful to determine the optimal receptor concentration for successful therapy.

CONCLUSION

Limited resolution and recovery of single-photon imaging techniques can result in undetected tumors or metastases when neuroendocrine tumors are imaged with ^{111}In-octreotide. Therefore, we attempted to enhance the possibilities of octreotide by substituting for ^{111}In its positron-emitting analog ^{110m}In and the use of PET. ^{110m}In-DTPA-D-Phe^1-octreotide can be prepared using the OctreoScan kit and locally produced ^{110m}In. Phantom studies and a clinical imaging study show that PET with ^{110m}In-DTPA-D-Phe^1-octreotide can better detect small tumors and might be able to more accurately quantify tumor uptake than can ^{111}In-DTPA-D-Phe^1-octreotide and SPECT.

ACKNOWLEDGMENTS

We thank Dr. Sten Nilsson for his input, Dr. Ulrike Garske for helpful comments on the manuscript, Mimi Lidholm for preparation of the radiopharmaceuticals, and the staff at Uppsala University PET Centre and the Division of Oncological Nuclear Medicine at Uppsala University Hospital for assistance with the measurements. We also thank the staff of The Svedberg Laboratory for technical help. This study was supported by grants 3978-B97-01XBB and 3978-B98-02XBB from the Swedish Cancer Society.

REFERENCES

1. Pauwels EKJ, McCready VR, Stoot JHMB, van Deurzen DFP. The mechanism of accumulation of tumour-localising radiopharmaceuticals. *Eur J Nucl Med.* 1998;25:277–305.
2. Reubi JC, Maurer R, von Werder K, Torhorst J, Klijn JG, Lamberts SW. Somatostatin receptors in human endocrine tumours. *Cancer Res.* 1987;47:551–558.
3. Bakker WH, Krenning EP, Breeman WA, et al. Receptor scintigraphy with a radioiodinated somatostatin analogue: radiolabeling, purification, biologic activity and in vivo application in animals. *J Nucl Med.* 1990;31:1501–1509.
4. Anderson CJ, Pajeau TS, Edwards WB, Sherman ELC, Rogers BE, Welch MJ. In vitro and in vivo evaluation of copper-64-octreotide conjugates. *J Nucl Med.* 1995;26:2315–2325.
5. De Jong M, Bakker WH, Krenning EP, et al. Yttrium-90 and indium-111 labelling, receptor binding and biodistribution of [DOTA^0, D-Phe^1, Tyr^3] octreotide, a promising somatostatin analogue for radionuclide therapy. *Eur J Nucl Med.* 1997;24:368–371.
6. De Jong M, Breeman WA, Bernard BF, et al. Evaluation in vitro and in rats of ^{161}Tb-DTPA-octreotide, a somatostatin analogue with potential for intraoperative scanning and radiotherapy. *Eur J Nucl Med.* 1995;22:608–616.
7. Krenning EP, Bakker WH, Kooij PP, et al. Somatostatin receptor scintigraphy with indium-111-DTPA-D-Phe-1-octreotide in man: metabolism, dosimetry and comparison with iodine-123-Tyr-3-octreotide. *J Nucl Med.* 1992;33:652–658.
8. Smith-Jones PM, Stolz B, Bruns C, et al. Gallium-67/gallium-68-[DFO]-octreotide: a potential radiopharmaceutical for PET imaging of somatostatin receptor-positive tumors—synthesis and radiolabeling in vitro and preliminary in vivo studies. *J Nucl Med.* 1994;35:317–325.
9. Krenning EP, Kwekkeboom DJ, Bakker WH, et al. Somatostatin receptor scintigraphy with [^{111}In-DTPA-D-Phe^1]- and [^{123}I-Tyr^3]-octreotide: the Rotterdam experience with more than 1000 patients. *Eur J Nucl Med.* 1993;20:716–731.
10. O'Byrne KJ, Carney DN. Radiolabelled somatostatin analogue scintigraphy in oncology. *Anticancer Drugs.* 1996;7:33–44.
11. Olsen JO, Pozderac RV, Hinkle G, et al. Somatostatin receptor imaging of neuroendocrine tumors with indium-111 pentetreotide (Octreoscan). *Semin Nucl Med.* 1995;25:251–261.
12. Tisell LE, Ahlman H, Wangberg B, et al. Somatostatin receptor scintigraphy in medullary thyroid carcinoma. *Br J Surg.* 1997;84:543–547.
13. Westlin JE, Janson ET, Arnberg H, Ahlstrom H, Oberg K, Nilsson S. Somatostatin receptor scintigraphy of carcinoid tumours using the [^{111}In-DTPA-D-Phe^1]-octreotide. *Acta Oncol.* 1998;32:783–788.
14. Adams S, Baum RP, Hertel A, Schumm-Draeger PM, Usadel KH, Hör G. Comparison of metabolic and receptor imaging in recurrent medullary thyroid carcinoma with histopathological findings. *Eur J Nucl Med.* 1998;25:1277–1283.
15. Lebtahi R, Cadiot G, Sarda L, et al. Clinical impact of somatostatin receptor scintigraphy in the management of patients with neuroendocrine gastroenteropancreatic tumors. *J Nucl Med.* 1997;38:853–858.
16. Chiti A, Fanti S, Savelli G, et al. Comparison of somatostatin receptor imaging, computed tomography and ultrasound in the clinical management of neuroendocrine gastro-entero-pancreatic tumours. *Eur J Nucl Med.* 1998;25:1396–1403.
17. Wester HJ, Brockmann J, Rösch F, et al. PET-pharmacokinetics of ^{18}F-octreotide: a comparison with ^{67}Ga-DFO- and ^{86}Y-DTPA-octreotide. *Nucl Med Biol.* 1997; 24:275–286.
18. Chu SYF, Ekström LP, Firestone RB. *WWW Table of Radioactive Isotopes*. Database version 1999-02-28. Available at: http://nucleardata.nuclear.lu.se/nucleardata/toi/. Accessed July 29, 2002.
19. Lundqvist H, Scott-Robson S, Einarsson L, Malmborg P. ^{110}Sn/^{110}In: a new generator system for positron emission tomography. *Appl Radiat Isot.* 1991;42: 447–450.
20. Lundqvist H, Tolmachev V, Bruskin A, Einarsson L, Malmborg P. Rapid separation of ^{110}In from enriched Cd targets by thermal diffusion. *Appl Radiat Isot.* 1995;46:859–863.
21. Bruskin A, Tolmachev V, Westlin JE, Lundqvist H. Separation of two labeled components of [^{111}In]-OctreoScan by HPLC. *J Radioanalytical Nucl Chem.* 2001;247:95–99.
22. Bergström M, Eriksson L, Bohm C, Blomqvist G, Litton J. Correction for scattered radiation in a ring detector positron camera by integral transformation of the projections. *J Comput Assist Tomogr.* 1983;7:42–50.
23. Links JM. Advances in nuclear medicine instrumentation: considerations in the design and selection of an imaging system. *Eur J Nucl Med.* 1998;25:1453–1466.
24. Ronga G, Salerno G, Procaccini E, et al. ^{111}In-Octreotide scintigraphy in metastatic medullary thyroid carcinoma before and after octreotide therapy: in vivo evidence of the possible down-regulation of somatostatin receptors. *Q J Nucl Med.* 1995;39:134–136.
25. Kaplan MS, Miyaoka RS, Kohlmyer SK, Haynor DR, Harrison RL, Lewellen TK. Scatter and attenuation correction for ^{111}In based on energy spectrum fitting. *Med Phys.* 1996;23:1277–1285.
26. Rota Kops E, Herzog H, Schmid A, Holte S, Feinendegen LE. Performance characteristics of an eight-ring whole body PET scanner. *J Comput Assist Tomogr.* 1990;14:437–445.
27. Kohlmyer SG, Miyaoka RS, Shoner SC, Lewellen TK, Eary JF. Quantitative accuracy of PET imaging with yttrium-86 [abstract]. *J Nucl Med.* 1999;40(suppl):280P.
28. Lubberink M. Quantitative imaging with PET: performance and applications of ^{76}Br, ^{52}Fe, ^{110m}In and ^{134}La [dissertation]. In: *Acta Universitatis Upsaliensis: Comprehensive Summaries of Uppsala Dissertations from the Faculty of Medicine.* Uppsala, Sweden: Uppsala University; 2001:1034.
29. Beattie BJ, Pentlow KS, Finn RD, Larson SM. A method for the removal of spurious activity in PET imaging introduced by cascade gamma rays [abstract]. *J Nucl Med.* 2001;42(suppl):201P.
30. De Jong M, Breeman WA, Bakker WH, et al. Comparison of ^{111}In-labeled somatostatin analogues for tumor scintigraphy and radionuclide therapy. *Cancer Res.* 1998;58:437–441.

31. Fjalling M, Andersson P, Forssell-Aronsson E, et al. Systemic radionuclide therapy using indium-111-DTPA-D-Phe[1]-octreotide in midgut carcinoid syndrome. *J Nucl Med.* 1996;37:1519–1521.
32. Tiensuu Janson E, Eriksson B, Öberg K, et al. Treatment with high dose [(111)In-DTPA-D-PHE1]-octreotide in patients with neuroendocrine tumors: evaluation of therapeutic and toxic effects. *Acta Oncol.* 1999;38:373–382.
33. Wänberg B, Nilsson O, Johanson V, et al. Somatostatin receptors in the diagnosis and therapy of neuroendocrine tumor. *Oncologist.* 1997;2:50–58.
34. Rösch F, Herzog H, Plag C, et al. Radiation doses of yttrium-90 citrate and yttrium-90 EDTMP as determined via analogous yttrium-86 complexes and positron emission tomography. *Eur J Nucl Med.* 1996;23:958–966.
35. Flower MA, Al-Saadi A, Harmer CL, McCready R, Ott RJ. Dose-response study in thyrotoxic patients undergoing positron emission tomography and radioiodine therapy. *Eur J Nucl Med.* 1994;21:531–536.
36. Pentlow KS, Graham MC, Lambrecht RM, Cheung NKV, Larson SM. Quantitative imaging of I-124 using positron emission tomography with applications to radioimmunodiagnosis and radioimmunotherapy. *Med Phys.* 1991;18:357–366.
37. Herzog H, Rosch F, Stocklin G, Lueders C, Qaim SM, Feinendegen LE. Measurement of pharmacokinetics of yttrium-86 radiopharmaceuticals with PET and radiation dose calculation of analogous yttrium-90 radiotherapeutics. *J Nucl Med.* 1993;34:2222–2226.
38. Kolbert KS, Sgouros G, Scott AM, et al. Implementation and evaluation of patient-specific three-dimensional internal dosimetry. *J Nucl Med.* 1997;38:301–308.
39. Tagesson M, Ljungberg M, Strand SE. A Monte-Carlo program converting activity distributions to absorbed dose distributions in a radionuclide treatment planning system. *Acta Oncol.* 1996;35:367–372.
40. Reubi JC. Neuropeptide receptors in health and disease: the molecular basis for in vivo imaging. *J Nucl Med.* 1995;36:1825–1835.

JNM The Journal of NUCLEAR MEDICINE

^{110m}In-DTPA-d-Phe^{1}-Octreotide for Imaging of Neuroendocrine Tumors with PET

Mark Lubberink, Vladimir Tolmachev, Charles Widström, Alexander Bruskin, Hans Lundqvist and Jan-Erik Westlin

J Nucl Med. 2002;43:1391-1397.

The Journal of Nuclear Medicine is published monthly.
SNMMI | Society of Nuclear Medicine and Molecular Imaging
1850 Samuel Morse Drive, Reston, VA 20190.
(Print ISSN: 0161-5505, Online ISSN: 2159-662X)

SNMMI SOCIETY OF NUCLEAR MEDICINE AND MOLECULAR IMAGING